

A LOCAL EDDY VISCOSITY MODEL FOR TURBULENT SHEAR FLOW

By Paul J. Ortwerth, Douglas C. Rabe,
and Donald P. McErlean
Air Force Aero Propulsion Laboratory
Wright-Patterson AFB, Ohio

INTRODUCTION

Turbulent flow fields are generated in shear flows of sufficiently high Reynolds number for which the laminar shear layer is unstable. Mean flow kinetic energy is transformed into a random turbulent kinetic energy and finally dissipated into random thermal energy. The present theoretical model attempts to make predictions of turbulent flow fields by using the historically popular eddy viscosity concept.

The eddy viscosity is assumed to be a fluid property dependent on the state of the fluid locally, namely the local density, turbulent kinetic energy, turbulence scale, and Mach number. An empirical law was found (ref. 1) which related eddy viscosity to these properties satisfactorily for free jets. This law is used without modification for the present set of test cases in free shear layers, free-jet decay, coaxial mixing, and wakes.

At present the scale of turbulence is taken as a constant at any axial location equal to the width of the shear layer.

By utilizing the boundary-layer order-of-magnitude analysis, a coupled set of fluid dynamic equations is formulated, which of necessity includes the equation for the production of turbulent kinetic energy.

SYMBOLS

\bar{c}_p mean specific heat at constant pressure

d jet diameter

def $\bar{\mathbf{U}} = \bar{\nabla}\bar{\mathbf{U}} + (\bar{\nabla}\bar{\mathbf{U}})^*$, where $(\bar{\nabla}\bar{\mathbf{U}})^*$ is the transpose of $\bar{\nabla}\bar{\mathbf{U}}$

d_k rate of dissipation of turbulence kinetic energy into random thermal energy

\bar{h} mean static enthalpy

\bar{h}_i	species enthalpy
$\bar{\mathbf{I}}$	identity tensor
k	turbulence kinetic energy, $\frac{1}{2} \left[\overline{(\rho U)'U'} + \overline{(\rho V)'V'} + \overline{(\rho W)'W'} \right]$
L_D	scale of large eddies
M	local Mach number
N_{Pr}	mean Prandtl number
$N_{Pr,T}$	turbulent Prandtl number, 0.75
N_{Sc}	Schmidt number, 0.75
$N_{Sc,T}$	turbulent Schmidt number
p_e	static pressure at edge of shear layer in the nonturbulent region
p_T	turbulence pressure
\bar{p}	mean static pressure
r	radial coordinate
r_0	jet radius
T_t	total temperature
$T_{t,0}$	initial total temperature
\bar{T}	mean static temperature
U	streamwise velocity
U_e	velocity at edge of shear layer
U_0	initial velocity

U_1	velocity on high-velocity side of shear layer
U_2	velocity on low-velocity side of shear layer
V	normal velocity
$W = 1 - \frac{U}{U_e}$	
x	streamwise coordinate for two-dimensional shear layers
y	coordinate normal to shear layer for two-dimensional shear layer
α_i	mass fraction of species i
ϵ_k	kinematic diffusivity for turbulent kinetic energy, $\rho\epsilon_k = \mu_T$
μ_T	eddy viscosity
$\bar{\mu}$	mean molecular viscosity coefficient
ρ	density
ρ_1	density on high-velocity side of shear layer
ρ_2	density on low-velocity side of shear layer
σ	shear layer spreading parameter
σ_0	incompressible spreading parameter for $\frac{U_2}{U_1} = 0$
$\bar{\tau}_T$	Reynolds stress tensor, $\overline{(\rho\bar{U})' \bar{U}'}$
ψ	stream function (subscripts r and x indicate derivatives with respect to radius and streamwise coordinate, respectively)

EQUATIONS

The equations are presented in cylindrical coordinates.

Reynolds stresses

The turbulence stresses are formulated in the following manner:

$$\bar{\tau}_T = -p_T \bar{I} + \mu_T \text{def } \bar{U} \quad (1)$$

separating the turbulence stress tensor into static pressure and shear stress tensor.

Turbulence pressure is by definition

$$p_T = \frac{2}{3} \rho k \quad (2)$$

Turbulent kinetic energy

The turbulent shear stress and pressure are coupled to the turbulent kinetic energy by the following equation:

$$\frac{1}{r} \frac{\partial}{\partial r} (r \bar{\rho} \bar{V} k) + \frac{\partial}{\partial x} (\bar{\rho} \bar{U} k) = -p_T \frac{\partial \bar{U}}{\partial x} + \mu_T \left(\frac{\partial \bar{U}}{\partial r} \right)^2 + \frac{1}{r} \frac{\partial}{\partial r} \left(r \bar{\rho} \epsilon_k \frac{\partial k}{\partial r} \right) - d_k \quad (3)$$

Eddy viscosity

Following reference 1, the equations for eddy viscosity, dissipation, and scale are

$$\mu_T = \bar{\rho} \frac{L_D}{16.5} \left(\frac{2}{3} k \right)^{1/2} \left(\frac{\epsilon}{\epsilon_0} \right) \quad (4)$$

$$L_D = \frac{\bar{U}_{\max} - \bar{U}_{\min}}{\left(\frac{\partial \bar{U}}{\partial r} \right)_{\max}} \sqrt{2} \quad (5)$$

and

$$d_k = \frac{3}{2} \bar{\rho} \frac{\left(\frac{2}{3} k \right)^{3/2}}{L_D} \quad (6)$$

where

$$\frac{\epsilon}{\epsilon_0} = 1 - M^2 \quad (0 \leq M \leq 0.6)$$

or

$$\frac{\epsilon}{\epsilon_0} = (1 + 0.25M)^{-2} \quad (0.6 \leq M < \infty) \quad (7)$$

Continuity

$$\frac{1}{r} \frac{\partial}{\partial r} (r \bar{\rho} \bar{V}) + \frac{\partial}{\partial x} (\bar{\rho} \bar{U}) = 0 \quad (8)$$

Radial momentum integral

$$\bar{p} + p_T = p_e \quad (9)$$

Streamwise momentum equation

$$\frac{1}{r} \frac{\partial}{\partial r} (r \bar{\rho} \bar{V} \bar{U}) + \frac{\partial}{\partial x} (\bar{\rho} \bar{U} \bar{U}) = - \frac{\partial p_e}{\partial x} + \frac{1}{r} \frac{\partial}{\partial r} \left[r (\bar{\mu} + \mu_T) \frac{\partial \bar{U}}{\partial r} \right] \quad (10)$$

Energy equation

$$\begin{aligned} \bar{\rho} \bar{V} \frac{\partial \bar{h}}{\partial r} + \bar{\rho} \bar{U} \frac{\partial \bar{h}}{\partial x} = \bar{U} \frac{\partial \bar{p}}{\partial x} + d_k + \bar{\mu} \left(\frac{\partial \bar{U}}{\partial r} \right)^2 + \frac{1}{r} \frac{\partial}{\partial r} \left[r \left(\frac{\bar{\mu}}{N_{Pr}} + \frac{\mu_T}{N_{Pr,T}} \right) \bar{c}_p \frac{\partial \bar{T}}{\partial r} \right] \\ + \frac{1}{r} \frac{\partial}{\partial r} \left[r \left(\frac{\bar{\mu}}{N_{Sc}} + \frac{\mu_T}{N_{Sc,T}} \right) \sum \bar{h}_i \frac{\partial \alpha_i}{\partial r} \right] \end{aligned} \quad (11)$$

Species continuity

$$\frac{1}{r} \frac{\partial}{\partial r} (r \bar{\rho} \bar{V} \alpha_i) + \frac{\partial}{\partial x} (\bar{\rho} \bar{U} \alpha_i) = \frac{1}{r} \frac{\partial}{\partial r} \left[r \left(\frac{\bar{\mu}}{N_{Sc}} + \frac{\mu_T}{N_{Sc,T}} \right) \frac{\partial \alpha_i}{\partial r} \right] \quad (12)$$

Numerical solution of these equations follows Edelman and Fortune (ref. 2).

The equations are transformed by the Von Mises transformation as

$$\left. \begin{aligned} X &= x \\ \psi \psi_r &= \bar{\rho} \bar{U} r \\ \psi \psi_X &= -\bar{\rho} \bar{V} r \\ a &= \frac{\mu \bar{\rho} \bar{V} r}{\psi} \end{aligned} \right\} \quad (13)$$

Then the finite-difference equations are formed by using the following substitutions:

Partial derivative in the X-direction

$$\frac{(\phi_{n+1,m} - \phi_{n,m})}{\Delta X} = \frac{\partial \phi}{\partial X} \quad (14)$$

Partial derivative in the ψ -direction

$$\frac{(\phi_{n,m+1} - \phi_{n,m-1})}{2 \Delta \psi} = \frac{\partial \phi}{\partial \psi} \quad (15)$$

Second derivative in the ψ -direction

$$\frac{a_{n,m}}{\Delta\psi^2} (\phi_{n,m+1} - 2\phi_{n,m} + \phi_{n,m-1}) + \frac{1}{4} \frac{1}{\Delta\psi^2} (\phi_{n,m+1} - \phi_{n,m-1})(a_{n,m+1} - a_{n,m-1}) = \frac{\partial}{\partial\psi} \left(a \frac{\partial\phi}{\partial\psi} \right) \quad (16)$$

Further discussion of these equations can be found in reference 1.

RESULTS

Numerical results have been obtained for each of the categories. For each problem an initial turbulence kinetic energy profile and scale are needed in addition to a velocity and temperature profile. These data on turbulence were not supplied and were estimated. This was not a serious problem for the test cases for free shear layers; however, initial turbulence level is important for the decay of free jets and coaxial jets, and free-stream turbulence is important to the decay of wakes. In the spirit of making predictions, no attempt was made to "fit" the solutions to the data by reinitializing those problems which did not work well. In fact, comparisons were not made until all cases were run.

Two-Dimensional Shear Layers

Test cases 1, 2, and 3.- Linear velocity profiles (figs. 1, 2, and 3) and a 1-percent turbulence intensity were used as input, and computations were started with 14 data points in ψ -direction. The initial shear layers were a few centimeters thick, and computations carried out 10 meters (30 ft) in the downstream direction.

Test cases 4 and 5.- The given profiles (figs. 4 to 8) and an initial turbulence intensity of 1 percent of U_1 were used to initialize the problems. The initial number of points in the ψ -direction were 16 and 19 for cases 4 and 5, respectively. For test case 4, the profiles were shifted so that a velocity ratio of 0.5 occurred at $y = 7$ cm (3 in.). For case 5, the 0.5 velocity ratio was shifted to $y = 2.5$ cm (1.0 in.).

Free Jets

Test case 7.- The given profile (figs. 9 and 10) was input with a 1-percent turbulence intensity by using 14 initial points in the ψ -direction. The theoretical points seem to have more scatter than the data points. This may be due to the nature of the ϵ/ϵ_0 function used in equation (7).

Test case 8.- This problem was started downstream at $x/d = 2.79$ by using the given profile (fig. 11) and assuming a self-similar turbulence intensity in the shear layer and 15 initial points in the ψ -direction.

Coaxial Mixing

Test case 10.- The initial profiles (figs. 12 and 13) at $x/d = 2.966$ were used with a self-similar turbulence profile and 14 initial points in the ψ -direction. The potential core length is overpredicted in this problem, perhaps because of large initial turbulence levels in the jet and external stream. This problem is basically one of a free jet with an embedded coaxial jet. The outer shear layer may also have affected these data through acoustic radiation to the mixing zone.

Test case 11.- The initial profiles (fig. 14) and a 5-percent turbulence intensity were used as input. Thirty initial points were used in the ψ -direction to fit the profiles adequately. These initial profiles show that basically two shear layers are present - a feature not accounted for in the formulation of the theory where only one scale is used at a given axial location. The initial center-line behavior is adequately predicted but not the final or wakelike zone. The reason for this is not known.

Test case 12.- Fifteen points were used to describe the initial profiles (fig. 15) in the ψ -direction. An 8-percent turbulence intensity was used in the hydrogen boundary layer and a 3-percent initial turbulence intensity in the air boundary layer. Again the potential core length is overpredicted, and no definite reason can be offered to explain the discrepancy.

Wakes (Test Case 17)

Fourteen points were used to initialize the problem at the station $x/d = 17.0$. (See fig. 16.) An initial turbulence intensity of 6 percent on the center line varying to 1 percent in the free stream was used.

The prediction is an order of magnitude too low. The reason for such a large discrepancy between theory and data is not known. It appears that the physics employed in this model do not correspond to what occurred in the experiment or that some larger error exists in the programming.

RECOMMENDED EXPERIMENTATION

The achievement of rapid mixing is the goal of the propulsion engineer. Some ideas are proposed to achieve that goal. The instability of shear layers, be they laminar or turbulent, makes them capable of extracting power from various sources. The instability

of shear layers is not properly exploited by many devices except perhaps in whistles and musical instruments such as a flute or an organ.

Because of this instability, greatly enhanced mixing occurs, often leading to anomalous experimental results when not recognized. It is the authors' opinion that these exciting phenomena should be exploited more fully by the propulsion engineer. Figure 17 sketches some interesting examples of shear-layer instabilities producing enhanced mixing.

The addition of moving mechanical parts which act as triggers or amplifiers to shear layers is also possible. An example of this occurs when the vortex shedding frequency of a cylinder is equal to the frequency of cylinder oscillations.

REFERENCES

1. Ortwerth, Paul James: Mechanism of Mixing of Two Nonreacting Gases. AFAPL-TR-71-18, U.S. Air Force, Oct. 1971.
2. Edelman, R.; and Fortune, O.: An Analysis of Mixing and Combustion in Ducted Flows. AIAA Paper No. 68-114, Jan. 1968.

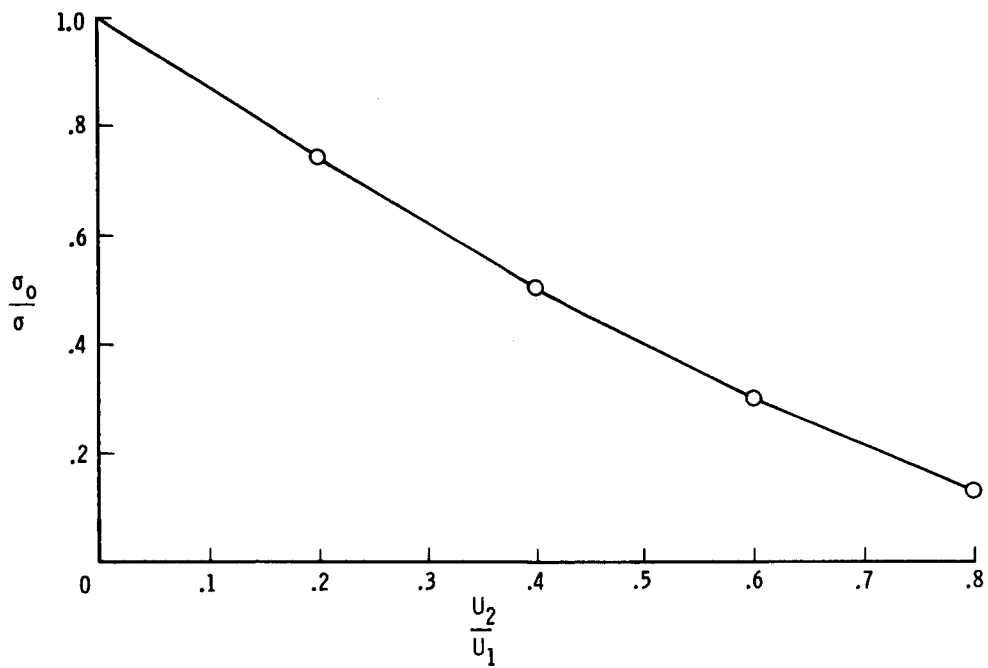


Figure 1.- Test case 1. $M = 0$.

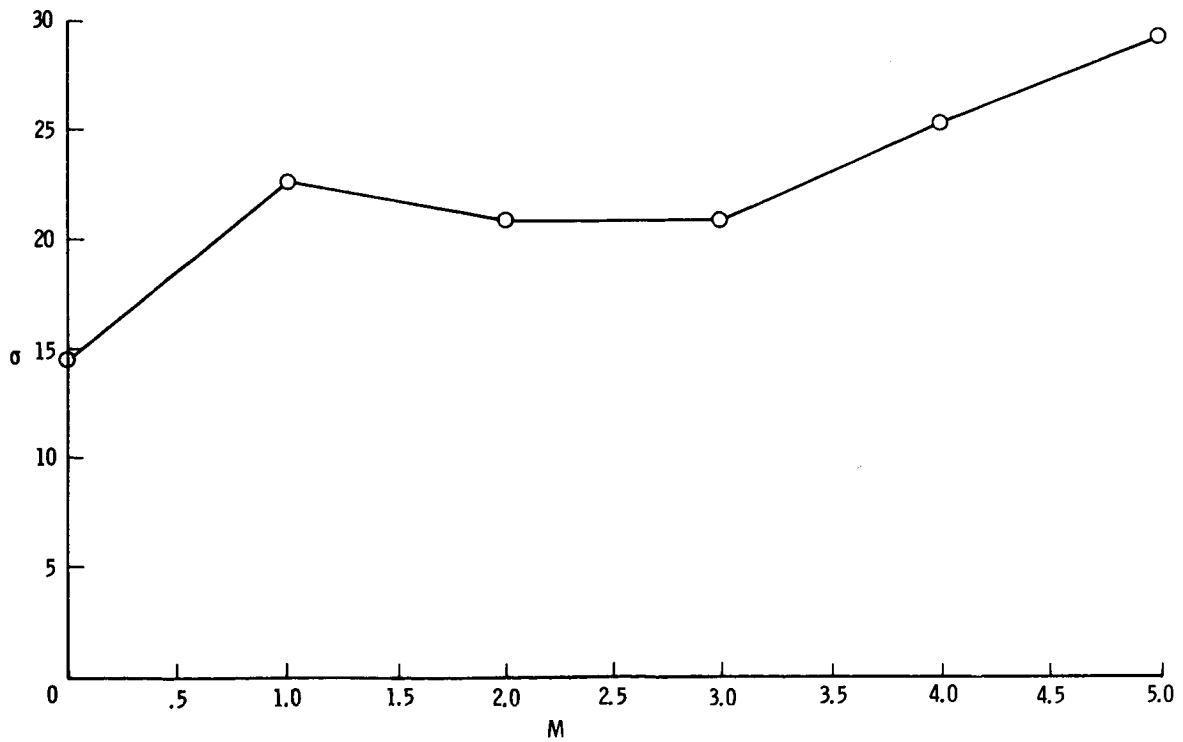


Figure 2.- Test case 2. $U_2/U_1 = 0.2$.

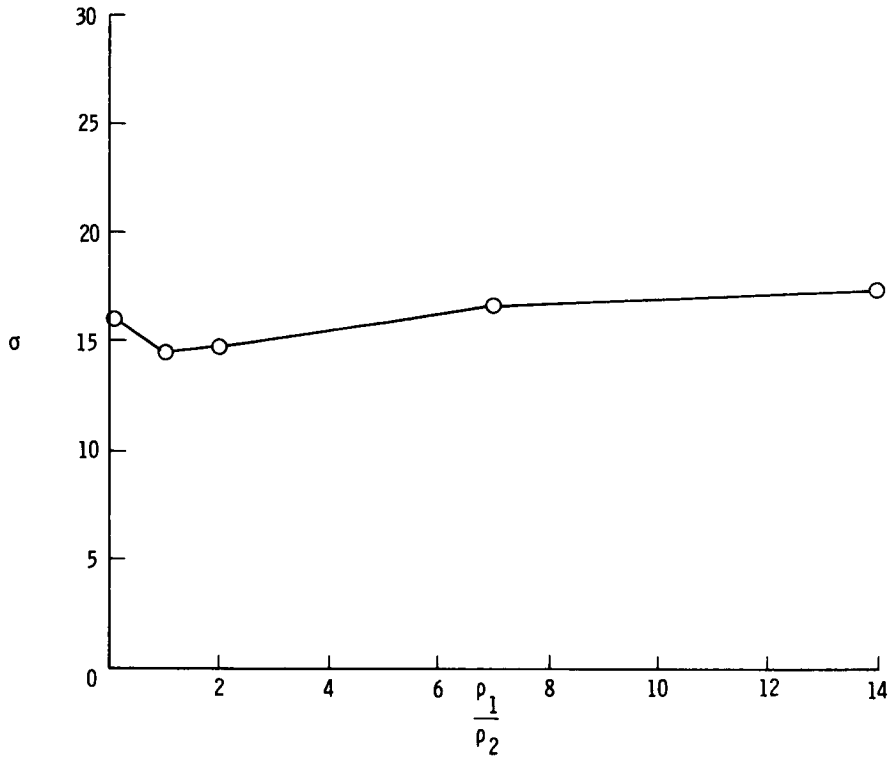


Figure 3.- Test case 3. $U_2/U_1 = 0.2$.

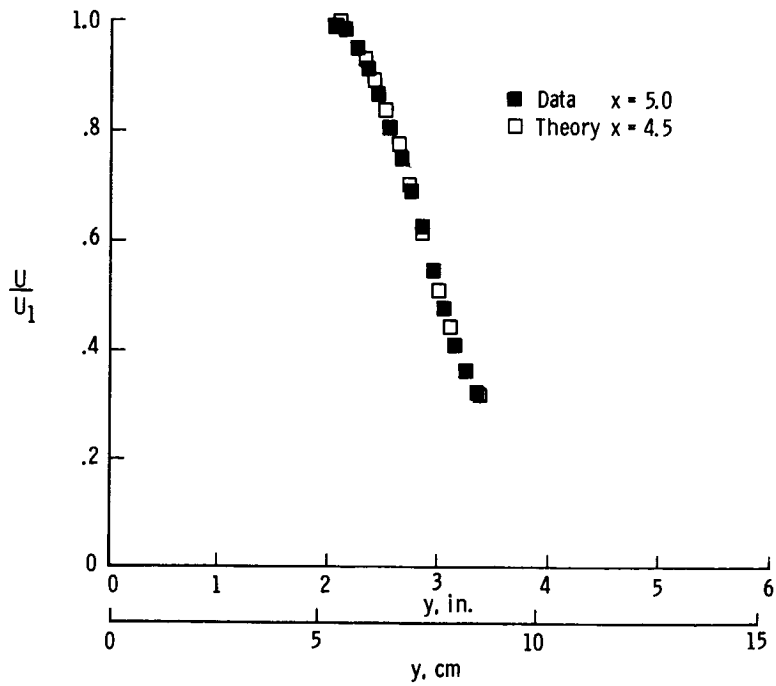


Figure 4.- Test case 4.

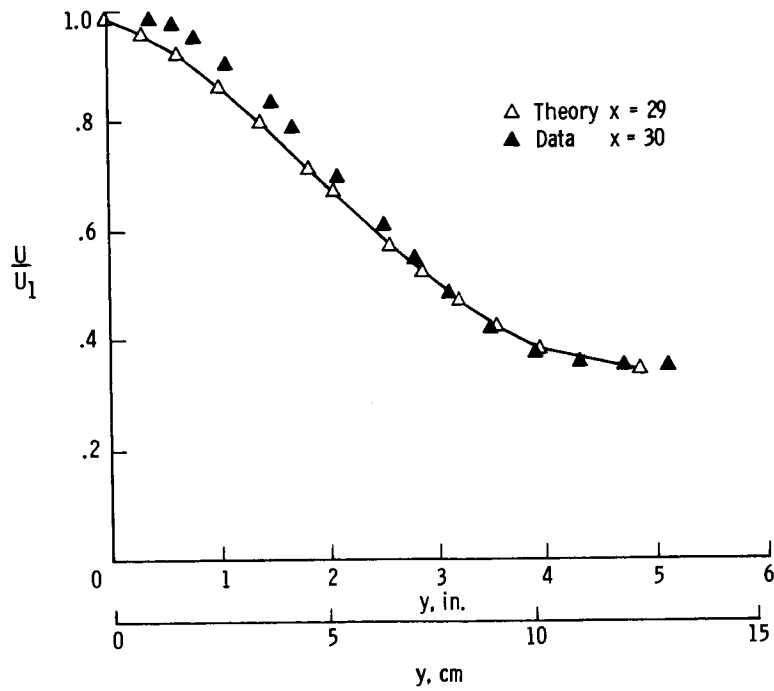


Figure 5.- Test case 4.

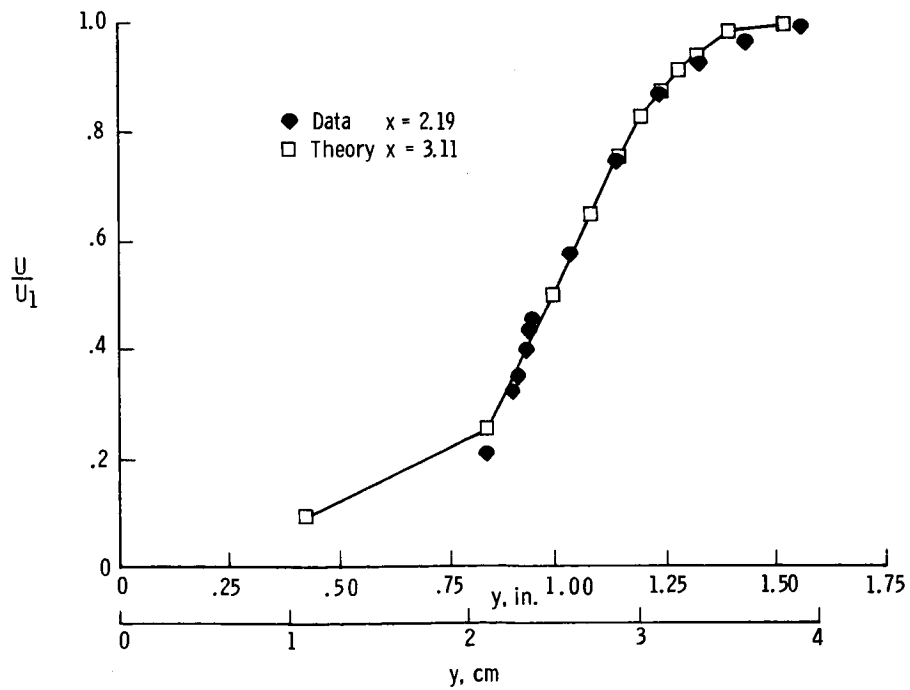


Figure 6.- Test case 5.

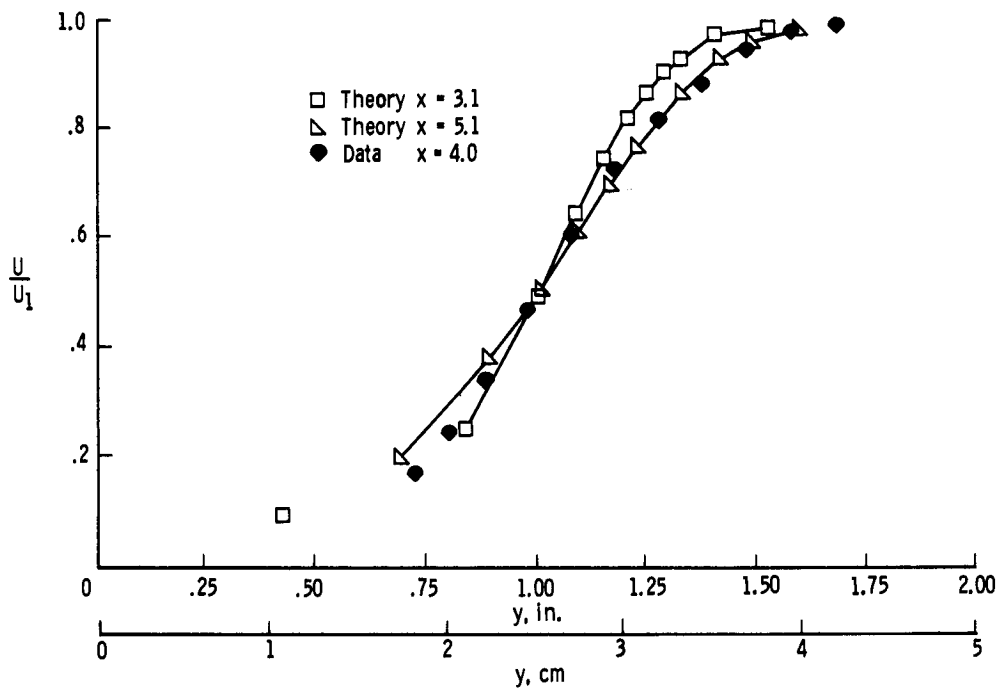


Figure 7.- Test case 5.

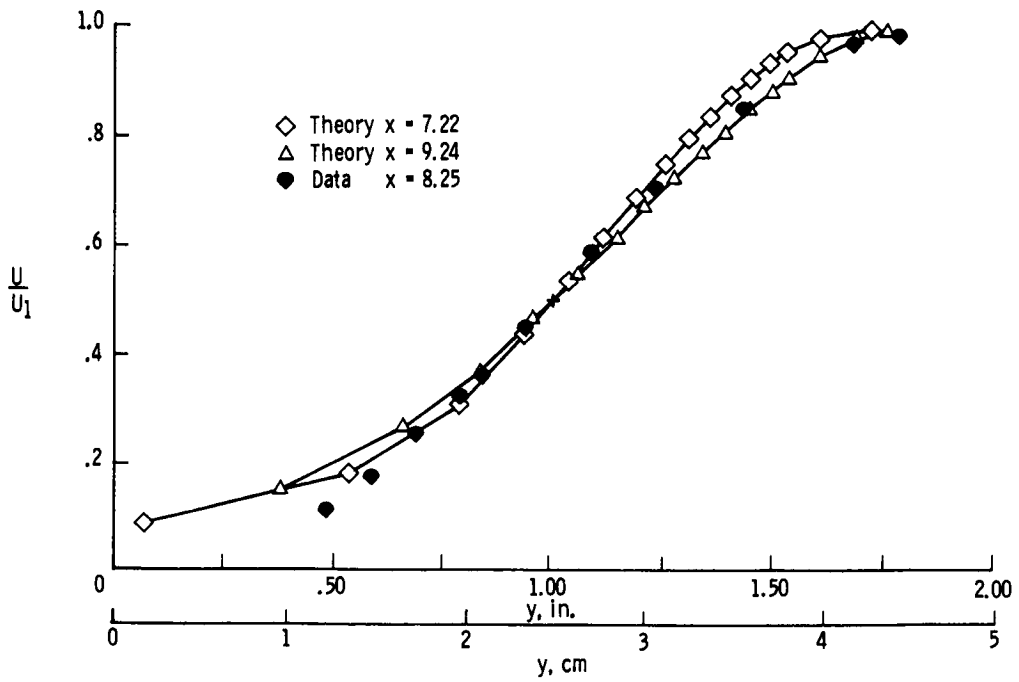


Figure 8.- Test case 5.

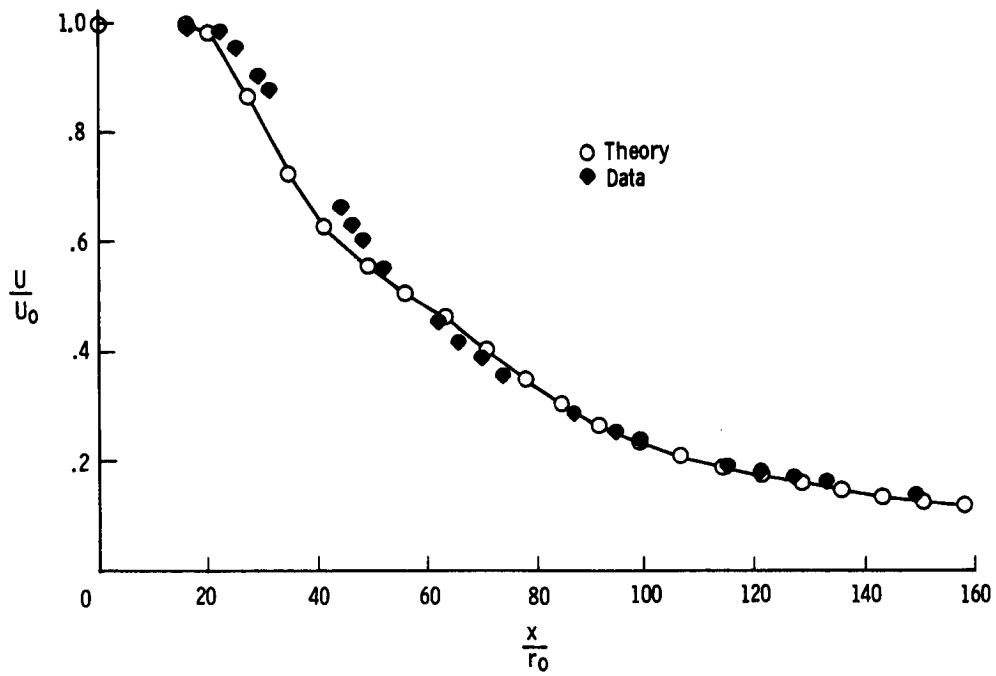


Figure 9.- Test case 7.

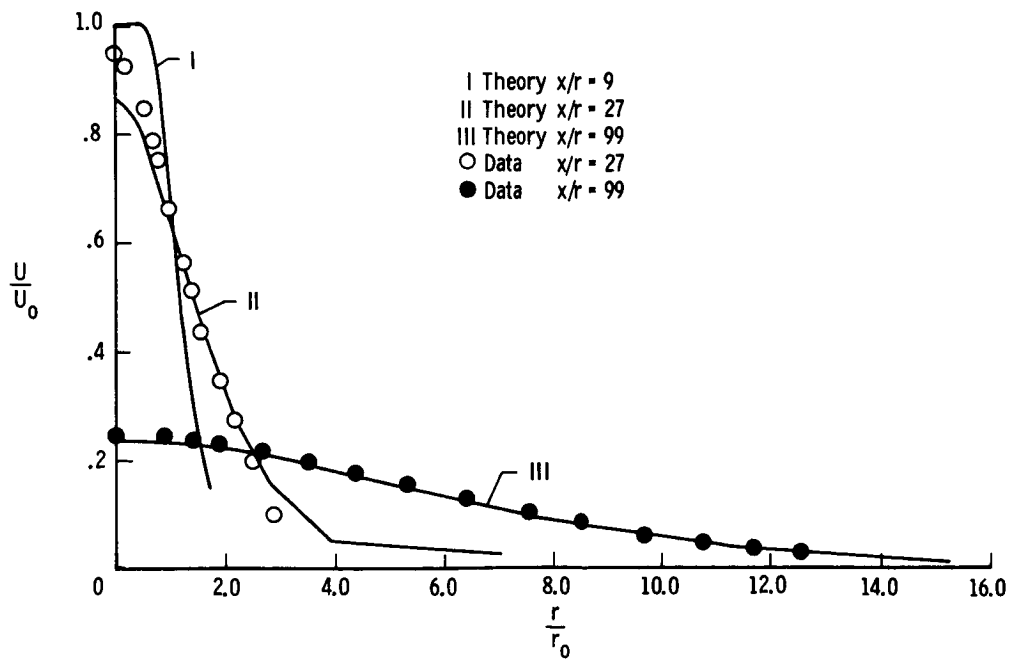


Figure 10.- Test case 7.

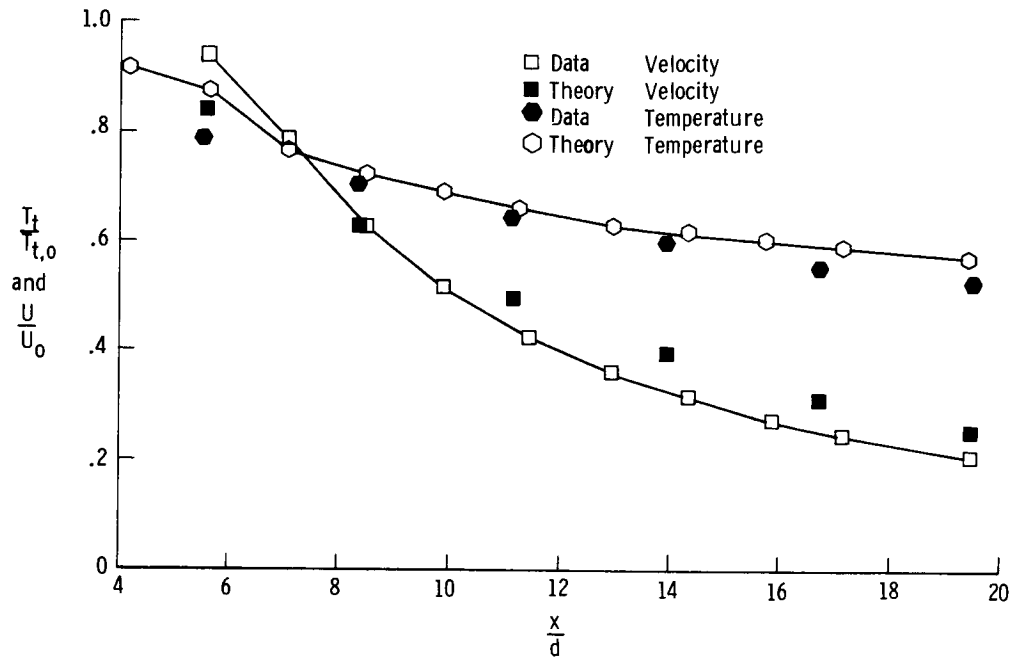


Figure 11.- Test case 8.

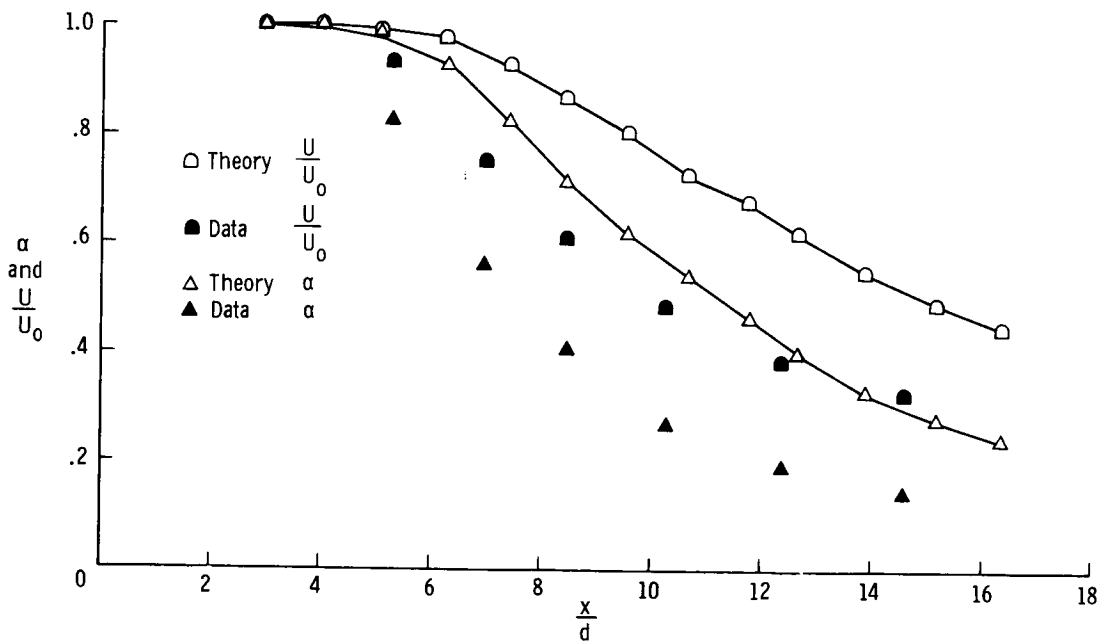


Figure 12.- Test case 10.

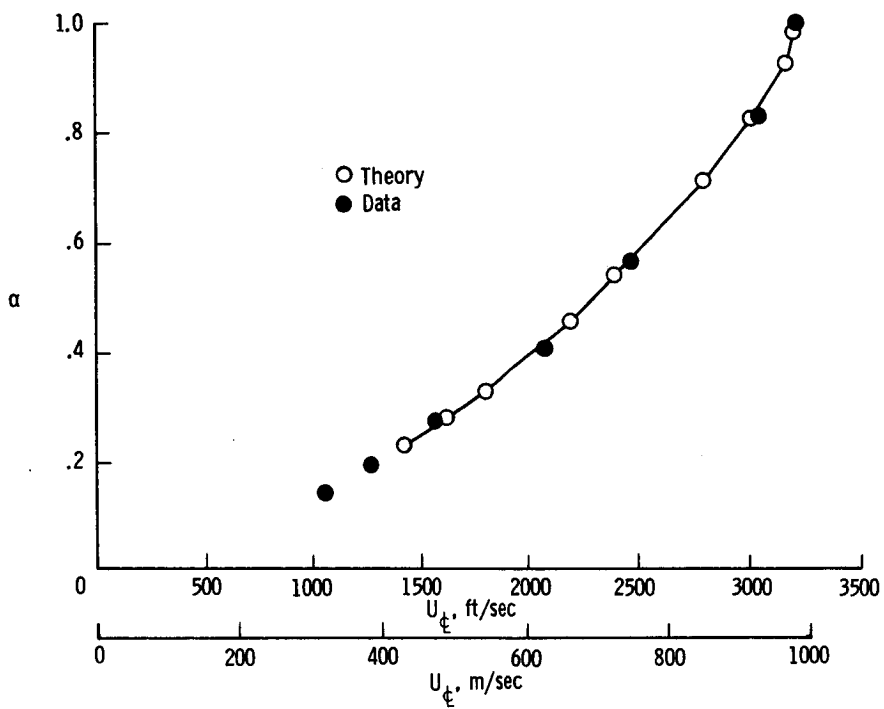


Figure 13.- Test case 10. Center-line variation of mass fraction and velocity.

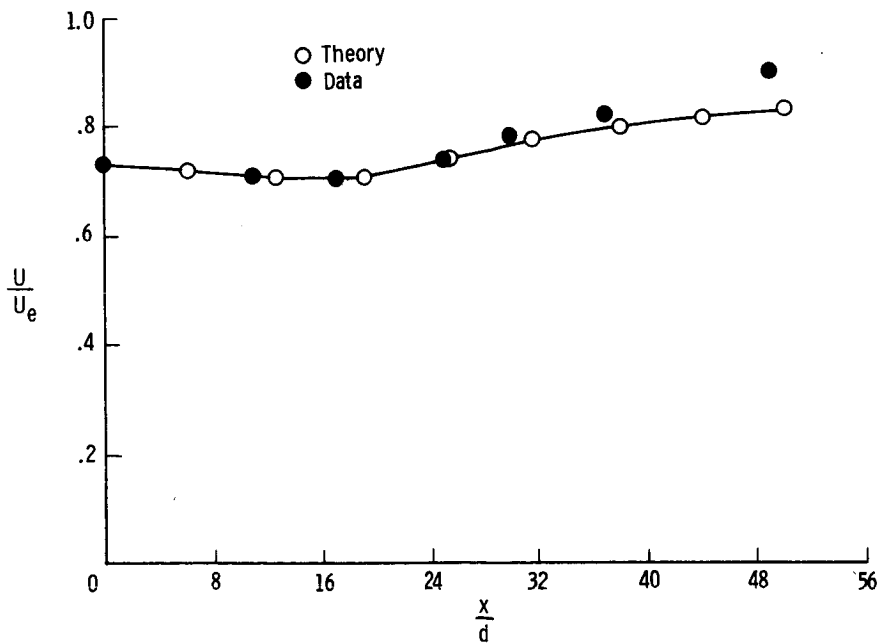


Figure 14.- Test case 11.

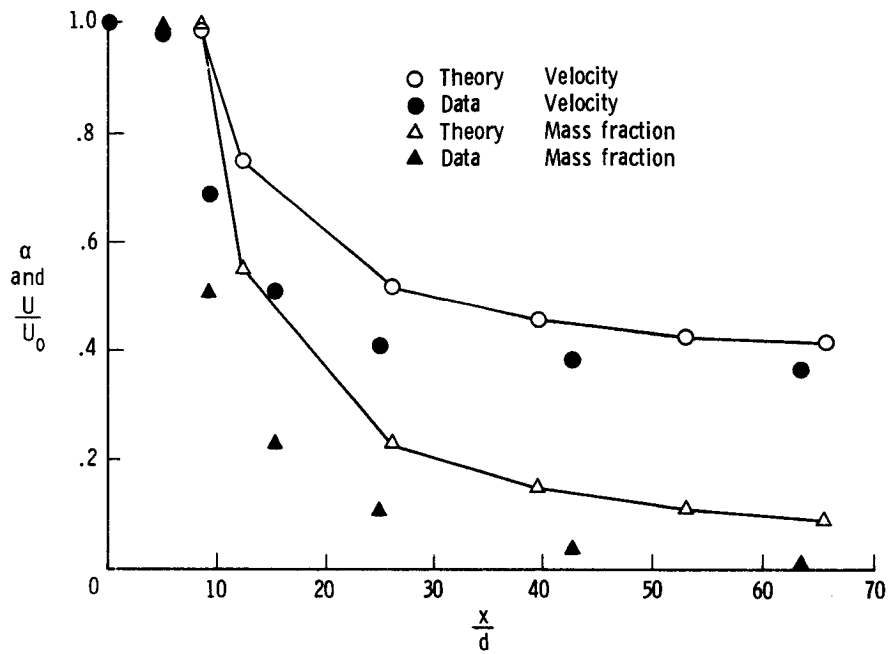


Figure 15.- Test case 12.

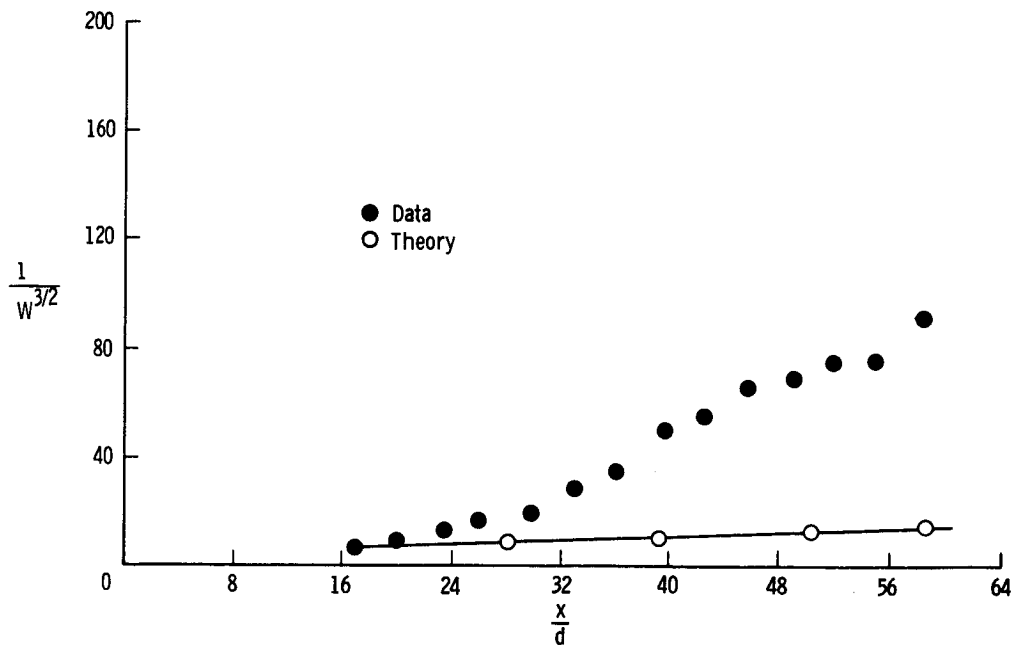
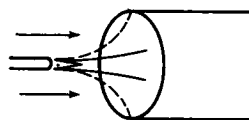


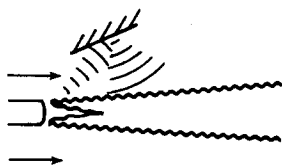
Figure 16.- Test case 17.



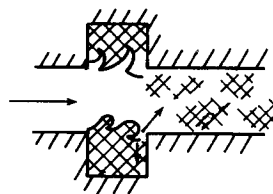
Periodic wakes
and jets



Singing flame



Acoustic beams



Cavity resonance

Figure 17.- Unsteady periodic mixing aids.

DISCUSSION

D. B. Spalding: Some of the plots of the axial concentration or axial velocity seem to show points which were rather far apart with straight lines drawn between them. Does that mean that you actually took very large forward steps in your computation?

P. J. Ortwerth: They were rather large but they weren't that large. That's how often the program printed out.

D. B. Spalding: What's your forward step size then as a fraction of width, for example?

P. J. Ortwerth: It's comparable to the step size in the radial direction. If you have 14 points, for example, across a shear layer, then you have to march forward with a little less than 1/14 of a shear layer in distance. So the curves are continuous; however, I really think that they are discontinuous enough that drawing straight lines between data points is not all that bad.

B. E. Launder: I noticed that when you showed your slide of the kinetic energy equation, that the first term on the right-hand side was, if memory serves me, something like, $2/3$ Density \times Turbulence energy \times Mean velocity gradient. Could you explain briefly the origin of that term?

P. J. Ortwerth: I assume that's equal to the turbulence normal stresses if you break the turbulent stress tensor into a normal part and a shear part like you would for a normal molecular flow or laminar flow of gas; that is $p_T \left(\frac{2}{3} \rho k \right)$ by definition.

B. E. Launder: Well, certainly if we were concerned with the normal stresses, I would agree with you, but the production in the turbulence energy equation is associated with shear stresses.

P. J. Ortwerth: That is right. I tried to point that out. If you, for example, have a combustion chamber with a gas velocity in there of 8000 ft/sec (2400 m/sec), and you have a turbulence intensity of 20 percent, this will correspond to an amount of energy, translated into gas temperature so you can understand it, of several thousand degrees. Now when you expand that gas through a nozzle, of course, there's a pressure gradient and a velocity gradient, and the normal turbulence shear stresses are such a large part of the pressure in the flow, that the work done pushing the gas out of the nozzle is significant. I want to know how much that is so I can integrate that equation with that term in there. As far as you're concerned, maybe it doesn't make any difference. In the normal incompressible flow those terms are very small.

W. A. Rodi: In reference to test case 17 you mention a possible Reynolds number influence. We found very similar predictions with our model where we do not introduce a function of one of the constants. I believe the reason for your bad predictions is that you

use a constant. In this particular case, the production of kinetic energy is very low, and that's why we get a very different constant. I believe that differences occur because we introduce this function of production over dissipation.

P. J. Ortwerth: Where I would have difficulty with that comment is if the production of turbulent energy is low, I wind up with a lower viscosity and with poorer agreement with the data.

W. A. Rodi: But, we introduced a function where the new constant would increase by a factor of about 5, and that's why we get better agreement.

P. J. Ortwerth: If I change the constant by a factor of 5, it probably would agree.